Description and Development of a SAW Filter CAD System

SAMUEL M. RICHIE, MEMBER, IEEE, BENJAMIN P. ABBOTT, MEMBER, IEEE, AND DONALD C. MALOCHA, SENIOR MEMBER, IEEE

Abstract—**This paper will present a description of the appropriate device models, design methods, and analysis techniques for a real-time surface acoustic wave (SAW) computer-aided design (CAD) system. The approaches presented have been successfully implemented in the creation of a fully integrated SAW filter CAD system for the design of bidirectional and three-phase unidirectional filters on a DEC VAX 11/750 system and for the design of bidirectional filters on an IBM PC-AT computer, which acts as an independent workstation. The focus of this paper will be on bidirectional transducer design and analysis using the PC-based computer system. CAD analysis of a SAW bidirectional filter will be compared to measured parameters.**

I. INTRODUCTION

THERE EXISTS a large base of knowledge on the design techniques and device physics for surface acoustic wave filter technology, which has led to a high degree of device model sophistication. Such device models allow for accurate prediction of each specific physical interaction in a SAW filter. Therefore, the integration of a set of compatible models for complete response calculation is possible. The implementation of such a set on a personal computer system would give the full realm of CAD benefits to the SAW filter engineer. These benefits include increased design and analysis productivity through reduced design and analysis cycle time, and greater accuracy of predictions through the ability to model higher order effects. Such a system would create a consistant or standardized model set which could lead to a better exchange of information among designers. Also, system engineers not familiar with the physical processes or details of the models could use the system to accurately design and analyze devices for system applications. This paper presents the development and implementation of a system for SAW bandpass filter design and analysis.

A basic schematic diagram for a SAW filter is shown in Fig. 1(a). Only a brief summary of the details of device design and analysis will be presented in this paper and the reader is referred to the references for more detailed descriptions [1]–[6]. The conventional SAW filter is composed of two bidirectional transducers on a piezoelectric substrate, either in direct cascade or separated by a multistrip coupler [7]. One or both of the transducers may be apodized, which allows for weighting of the electrodes by spatially changing overlaps in the acoustic beam [8]. An absorber is placed on either end of the crystal to eliminate the backward-traveling wave, which can cause spurious reflections. In addition to the acoustic response, analysis models must include the effects of the package parasitics and external electrical components. The block diagram for a conventional SAW filter is shown in Fig. 1(b), which includes the package effects and matching networks.

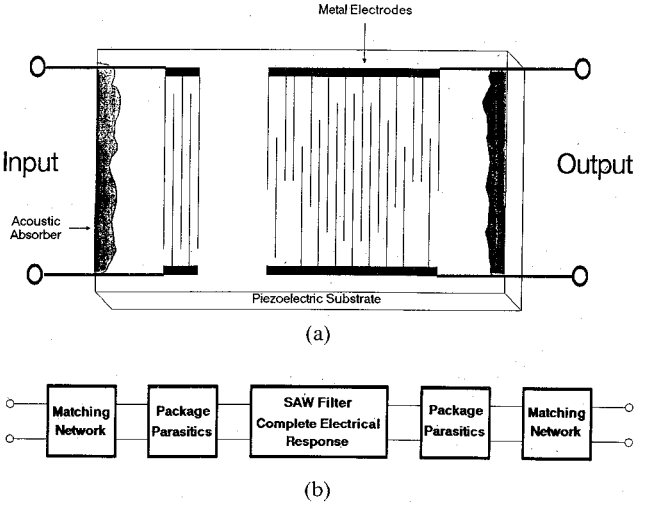

Fig. 1. (a) Basic schematic diagram showing a typical structure. (b) The corresponding functional block segmentation for the inclusion of all electrical effects.

A system option diagram for the PC-based workstation is shown in Fig. 2. The system contains all the CAD components necessary for a complete filter analysis and design-to-mask capability. Rather than present the specific system operation which has been developed, the focus of this paper is on the models chosen for analysis and synthesis. In order to maintain real-time analysis, the SAW transducer effects caused by bulk wave radiation, and transverse and longitudinal charge accumulation, SAW multimoding, diffraction, and mechanical edge reflections have been excluded from the models. Most operations in the analysis return a query to the designer within one minute. Comments on the algorithms used which enhance CAD speed while maintaining analysis accuracy will be

Manuscript received April 16, 1987; revised October 12, 1987. This work was supported in part by Andersen Laboratories, Bloomfield, CT, by the University of Central Florida's Engineering and Industrial Experiment Station, and by the University of South Florida's Microelectronics Design and Test Center.

The authors are with the Department of Electrical Engineering & Communication Sciences, University of Central Florida, Orlando, FL 32816.

IEEE Log Number 8718546.

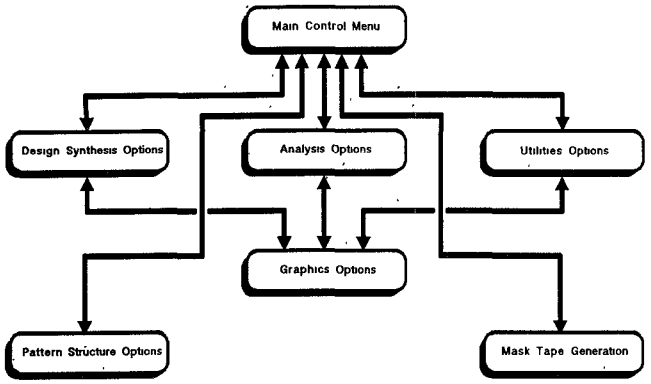

Fig. 2. SAW filter CAD system organizational flow diagram showing control flow between system functional options.

discussed. Finally, a comparison between an actual filter designed and analyzed on the PC workstation and measured results will be presented.

II. System Design Capabilities

The design of SAW filters most often begins with a frequency specification and less frequently with a time-domain specification (i.e., such as modulator filters). The design procedure requires finite time impulse response (FIR) implementations, and many procedures used in SAW filter design are similar to those used in digital filter design. The SAW filter requires the design of two interdigital transducers such that the acoustic device implementation produces the required overall transfer function. There are two principal design approaches:

1) Use a weighted transducer with an unweighted transducer.
2) Use two weighted transducers.

Approach 1 is very straightforward and applicable to all crystal cuts and filter bandwidths and is usually implemented with apodization weighting. Approach 2 can be implemented using phase-weighting techniques [9], [10] or by using a multistrip coupler with two apodized transducers on high coupling materials. For narrow-band filters on low-coupling materials, approach 2 can be implemented without the multistrip coupler by withdrawal weighting [11]–[13] one of the transducers. The designer chooses an approach based on many considerations, including device size, second-order effects, and fabrication issues. Fig. 3 shows a design session flow diagram for the CAD system. User inputs of the required frequency specifications generate a frequency template which can be viewed graphically. The user then chooses a suitable FIR synthesis approach which dictates the form of the parameters extracted from the frequency template. At this point, the calculation of the time samples for the transducer or filter is completed. The following discusses the FIR synthesis approaches used in the CAD system.

A filter synthesis technique based on the superposition of "eigen" triangles for the formation of an arbitrarily shaped filter function is one design option used in the CAD system [14], [15]. This approach uses a member of a

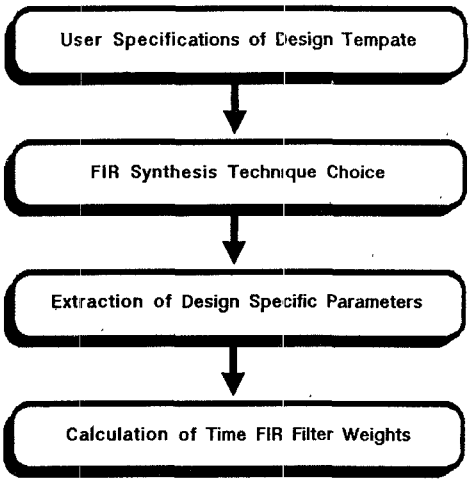

Fig. 3. SAW filter CAD system design procedure flow diagram.

cosine series which has a "near-triangle-shaped" frequency response with greater than 60 dB sidelobes. This particular function is expressed in time as

$$\begin{aligned} W(t,\tau) &= 0.44+0.5\cos(2\pi t/\tau) \\ &\quad +0.07\cos(4\pi t/\tau) && |t| \leqslant \tau/2 \\ W(t,\tau) &= 0 && |t| \geqslant \tau/2. \end{aligned} \quad (1)$$

The corresponding frequency-domain function $W(f)$ may also be obtained analytically using the frequency shift property of the Fourier transform. The passband is constructed using scaled and frequency-shifted functions, which can be written as $\beta \cdot W(f-f_i)$, and the filter transition bandwidth is determined by the time length τ. In a similar manner, the time-domain function is given analytically using superposition. This procedure allows completely arbitrary filter functions to be designed. A significant advantage of this technique is that is is noniterative, thus meeting the real-time requirement for the CAD system. It may also be used to synthesize multipassband responses, multilevel passsband responses, and nonsymmetric frequency responses. Typically this function is implemented on a single transducer, with the second transducer being a wide-band unweighted transducer.

In an analogous approach, the previously mentioned technique can be expanded by using an infinite set of cosine series functions to define the time response and can be used to synthesize arbitrary filter responses via superposition of time-domain functions [16], [17]. There are two functional time basis sets which are used, given by

$$\begin{aligned} h_{n1}(t) &= \sum_{n=0}^{N-1} a_n \cos[\omega_1(n)t]\,\mathrm{rect}(t/\tau) \\ h_{n2}(t) &= \sum_{n=0}^{N-1} b_n \cos[\omega_2(n)t]\,\mathrm{rect}(t/\tau) \end{aligned} \quad (2)$$

where $\omega_1(n) = 2n\pi/\tau$ and $\omega_2(n) = (2n+1)\pi/\tau$. The corresponding frequency response may be obtained analytically using the frequency shift property of the Fourier transform. Fig. 4 shows an example of the formation of a

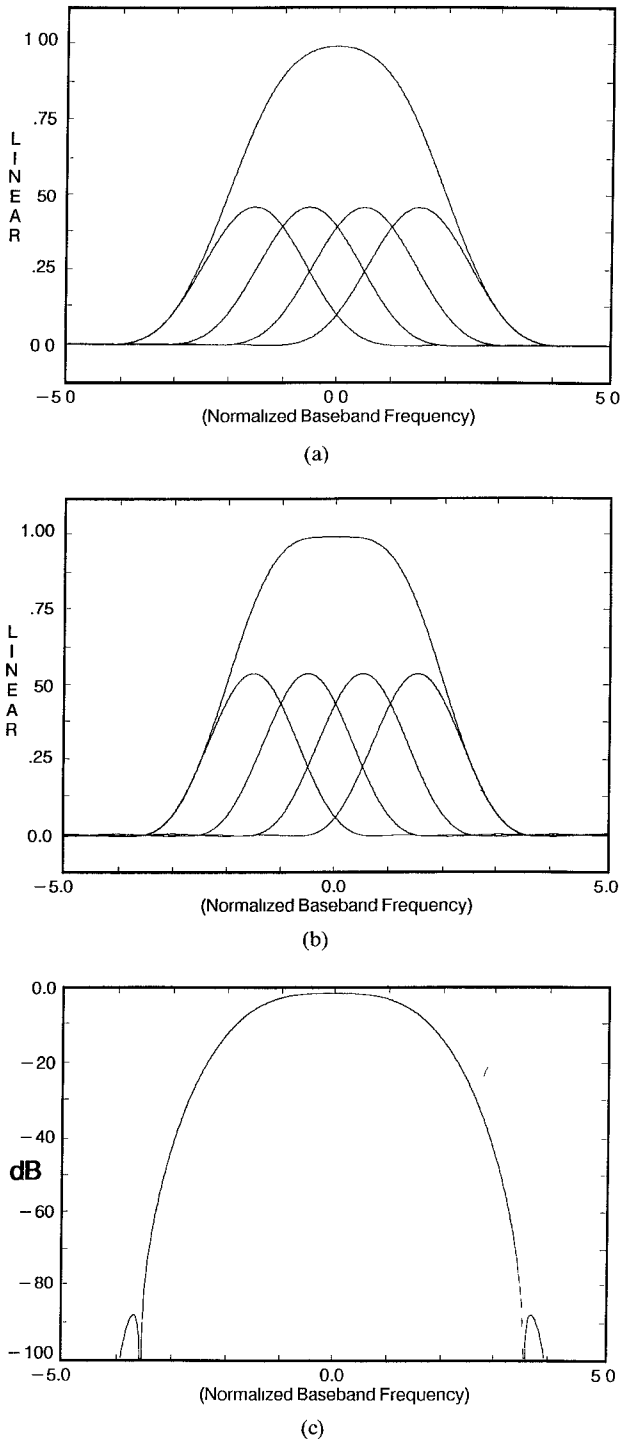

Fig. 4. Cosine series design example showing the synthesis of a passband function from (a) four even cosine series functions and (b) four odd cosine series functions. (c) Complete frequency response; product of (a) and (b).

passband frequency response from the sum of eight frequency-shifted and equally scaled cosine series frequency functions. Four cosine series functions are implemented in each of two separate transducer functions, as shown in Fig. 4. The complete filter transfer function is the product of the two transducer functions, as shown Fig. 4(c), which is plotted in dB. This technique has all of the advantages of the previous technique but with two greater advantages. First, the synthesized filter function can be separated into two orthogonal sets analytically, which can then be implemented, one each, on the two transducers which make up a SAW filter. This is a significant implementation ability which enhances the SAW filter's performance due to SAW filter structure considerations. Secondly, the filters time impulse response is near the minimum length as determined by the FIR Remez-exchange algorithm. This technique is noniterative, thus meeting the real-time requirement for the CAD system, and it may be used to synthesize multipassband, multilevel responses and nonsymmetric frequency responses.

The McClellan and Parks FIR filter synthesis approach [18]–[20], which uses the Remez-exchange algorithm for finding a minimal-length filter function from a set of frequency-domain specifications, is a popular design method for SAW filters; therefore its inclusion in the CAD system gives a complete set of design techniques. The major advantage of this approach is that the complete filter specifications, including all sidelobe levels, are considered during time impulse response function synthesis. The output of this technique is a minimal-order filter, and thus a minimal-length filter, which meets the filter specifications. This technique can be used to synthesize multipassband filters as well as filters with different sidelobe levels and transition bandwidths. The major disadvantage to this approach is its iterative calculation of the fiber function. This iterative approach can lead to very long filter synthesis times. In addition, polynomial zero extraction techniques must be used if the synthesized function is to be divided between two weighted transducers. This process is computer intensive and does not always yield realizable tap weights.

If two weighted SAW transducers are collinear on a device substrate and if the transducers are to be designed independently, then all the tap weights in one of the transducers must be either unity or zero. This weighting can be accomplished by implementing a square time pulse (rect$[t/\tau]$) or by withdrawal weighting [11], [12]. This technique yields a frequency function which is approximately equal to a desired narrow-band frequency function but has only time samples of unity. In this process, groups of small tap weights are summed and approximated by a single unity tap weight located at a position which is a function of the relative amplitudes and phases of the group of small weights. Fig. 5(a) shows a time FIR function, and the corresponding withdrawal weighted approximation is shown in Fig. 5(b). Fig. 5(c) shows the corresponding superimposed frequency responses. The narrow-band passband responses agree quite well but deviate significantly far from center frequency. Also, many implementations of multiphase SAW filter transducers use only uniform filter weights. Such considerations require the CAD system to include a withdrawal weighting module which can be used in conjunction with the other filter function synthesis techniques.

The authors prefer to use the cosine series FIR techniques because of their closed-form solutions and very

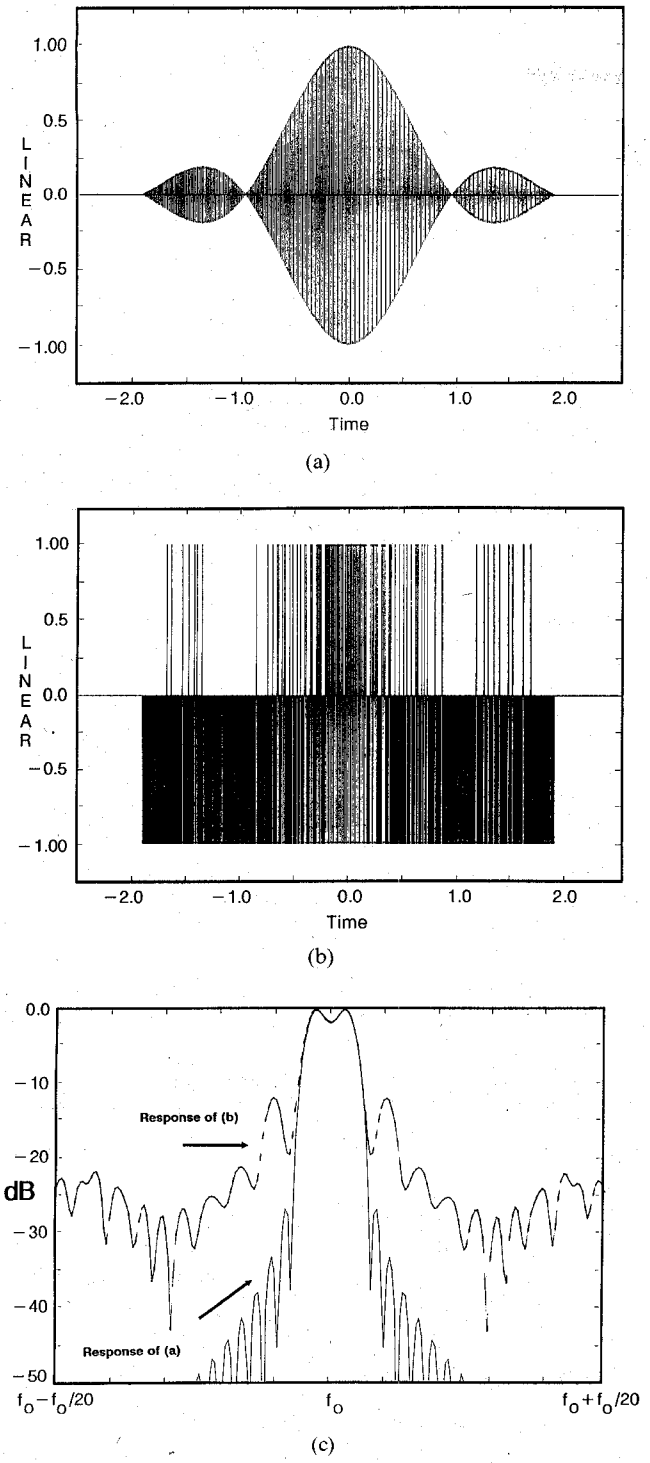

Fig. 5. Illustration of withdrawal weighting results showing (a) the original function, (b) the withdrawal weighted approximation, and (c) the two corresponding frequency responses.

rapid computer execution time (on the order of seconds). All time and frequency domain plots are available via the graphics options.

III. Transducer Analysis Techniques

In modeling the complete SAW filter response, the system can be divided into segments for ease in analysis and understanding. These segments are shown in the anal-

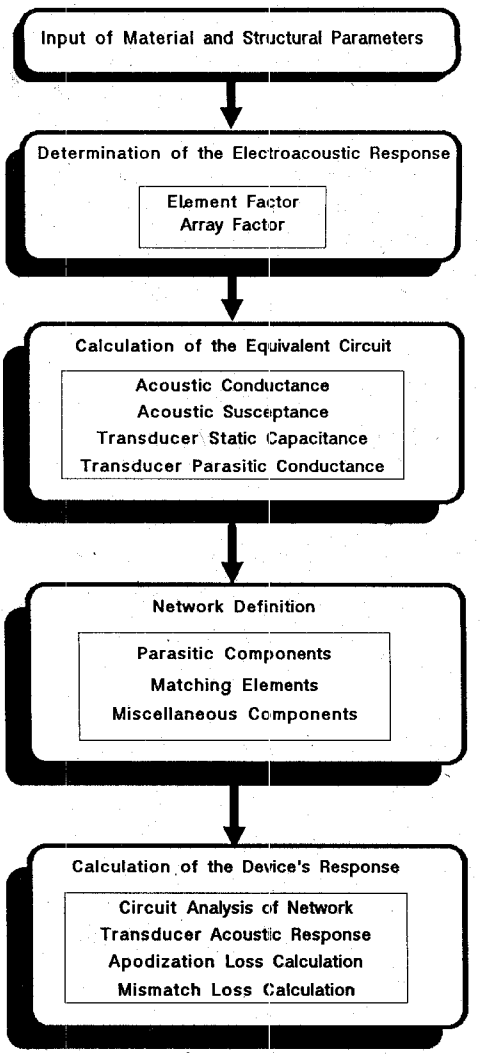

Fig. 6. SAW filter CAD system analysis procedure flow diagram.

ysis flow diagram of Fig. 6. A number of fundamental material parameters must be given which are a function of the piezoelectric material used, such as the coupling coefficient, and some basic device configuration information, such as the acoustic beam width. First, each of the two transducers is analyzed separately. In the analysis, the transducer equivalent circuit model is developed, which includes the static transducer capacitance, the acoustic conductance, and the Hilbert transform susceptance, as shown in Fig. 7. The transducers are modeled using the superposition analysis approach [3], [4], which assumes weak piezoelectric coupling. The wave potential is derived from the quasi-static charge distribution under the electrodes. The charge distribution can be analyzed as the convolution of an element factor, which is independent on the electrode width and periodicity, and an array factor, which is derived from the desired finite impulse response design. This modeling approach is both fast and accurate, which makes it a good candidate for CAD implementation.

For the analysis, it is necessary to derive and define the electroacoustic response. The surface wave potential gener-

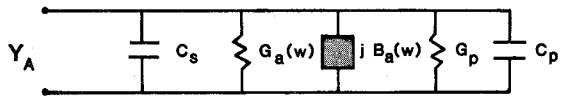

-Parasitic Conductance : G_p

-Static Parasitic Capacitive Susceptance : $B_p(w) = wC_p$

-Static Capacitive Susceptance : $B_c(w) = wC_s$

-Acoustic Conductance : $G_a(w)$

-Acoustic Susceptance : $B_a(w) = 1/\pi \int_{-\infty}^{\infty} \frac{Ga(w')}{w'-w}\, dw'$

-Single Port Admittance : $Y_a(w) = G_a(w) + G_p + j\,(B_c(w) + B_p(w) + B_a(w))$

-Transducer Q: $Q_o = \frac{B_c(w_o) + B_p(w_o)}{G_a(w_o) + G_p}$

Fig. 7. Lumped parameter equivalent circuit for a single SAW transducer with component calculation expressions.

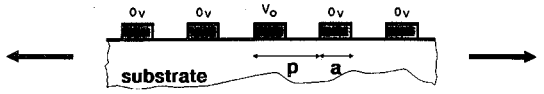

Fig. 8. Illustration of an infinitely long periodic transducer structure shown along a horizontal cross section.

ated by a SAW transducer has been shown to be closely related to the electrostatic charge distribution induced on the transducer by an incident electric potential [1], [21], [22]. This surface wave response of a transducer at a point x is stated analytically as

$$U_s(x,w) = jk^2 Q_e(\omega) e^{(j\beta x)} / (2 \cdot C_s) \tag{3}$$

where

- k^2 substrate coupling coefficient,
- Q_e electrostatic charge induced on the array,
- β wavenumber,
- x point at which the surface wave potential is to be evaluated,
- C_s $= \epsilon_0 + \epsilon_p$: the permitivity of free space and the piezoelectric substrate.

For the case of long transducers, the assumption that the transducer is infinite in extent greatly simplifies the analysis by allowing for the use of charge superposition. The element factor is expressed as the charge distribution present on the infinitely long transducer electrode array. An example transducer array is shown in Fig. 8.

The charge distribution has been solved analytically by Peach [23] and Datta and Hunsinger [4] and a plot is shown in Fig. 9. The spectral response of the element factor is given by

$$Q_f(\omega) = V_0 C_s \frac{2\sin(\pi s)}{P_{-s}[-\cos(\pi a/p)]} P_n[\cos(\pi a/p)],$$

$$n \leqslant \frac{\omega p}{2\pi v_s} \leqslant m+1 \tag{4}$$

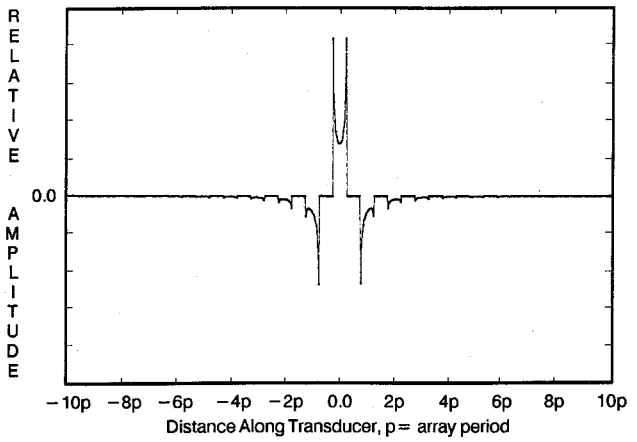

Fig. 9. Solution of the charge distribution for an infinitely long transducer array with a nonzero applied voltage to a single electrode with all other electrodes grounded.

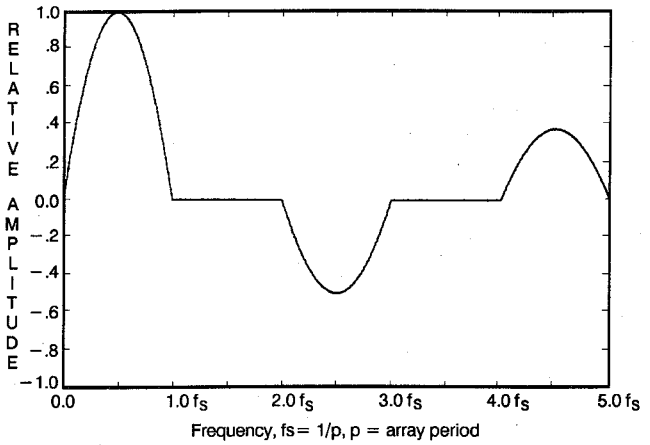

Fig. 10. Frequency response of the charge distribution for an infinitely long transducer array with a metallization ratio of 50 percent.

where

- a electrode width,
- p electrode period,
- $P_v(x)$ Legendre function with variable x and degree v,
- n integer portion of $\omega p/2\pi v_s$,
- s $= \omega p/2\pi v_s - n$,
- v_s surface wave velocity.

A plot of the element factor frequency response for $a/p = 0.5$ is shown in Fig. 10. The array factor describes the polarity sequence applied to the electrodes. The complete electrostatic charge distribution is therefore

$$q_e(x) = a_f(x) * q_f(x) \tag{5}$$

where

$$a_f(x) = \sum_{i=1}^{N} W_i(x - x_i). \tag{6}$$

In (6), W_i is the effective weight of the ith electrode centered at x_i. W_i is defined in terms of the polarity applied to the ith electrode, V_i, and the length of the ith

electrode L_i. The electrode length is generally normalized to the width of the beam:

$$W_i = V_i L_i. \tag{7}$$

In the implementation of SAW devices, the array factor may be modulated either by the polarity sequence applied to the electrodes, i.e., amplitude weighting, or by varying the lengths of the individual electrodes, i.e., apodization [8]. The most common form of weighting is apodization, and will be the only form of weighting considered here.

Equation (5) may be alternately expressed in the frequency domain as

$$Q_e(w) = A_f(w) \cdot Q_f(w). \tag{8}$$

For short arrays, for which charge superposition is not as accurate, the method of the Green's function may be used to determine the electrostatic charge distribution present on the transducer [24], [25]. Green's function is used to relate a sequence of potentials to a sequence of charges and is expressed as

$$v(x) = g(x) * q(x) = \int_{-\infty}^{+\infty} g(x-z) q(z)\, dz. \tag{9}$$

In discrete form (9) is expressed as

$$v_i = v_{\text{ref}} + \sum_{j=1}^{N} g_{i-j} q_j. \tag{10}$$

A reference has been added to the equations since only relative potentials are known. The reference voltage v_{ref} is the potential that would exist as x approaches negative infinity. For the case of the electrostatic transducer, the Green's function is stated as [24]

$$g(x) = -\ln |x| / C_s. \tag{11}$$

In discrete form g_{i-j} may be expressed in a normalized form as

$$g_{i-j} = d \ln |x_i - x_j| \tag{12}$$

where d is the width of each sampled point. Note that in the form of (12) a singularity exists in the discrete form of the Green's function for $x_i = x_j$. As a result, this form is not suitable for numerical analysis. A more satisfactory technique is to represent the discrete Green's function as an integral mean of $g(x_i - x_j)$ about x_j as

$$g_{i-j} = \int_{x_j - d/2}^{x_j + d/2} g(x_i - x)\, dx. \tag{13}$$

The result is a Green's function of the form,

$$g_{i-j} = |x_i - x_j| \cdot \ln |x_i - x_j + d/2| - |x_i - x_j| \cdot \ln |x_i - x_j - d/2| + d. \tag{14}$$

This simple form of the Green's function is very efficient in calculating the fundamental response of an array of electrodes.

Conservation of charge on the electrodes requires that

$$\sum_{i=1}^{N} q_i = 0. \tag{15}$$

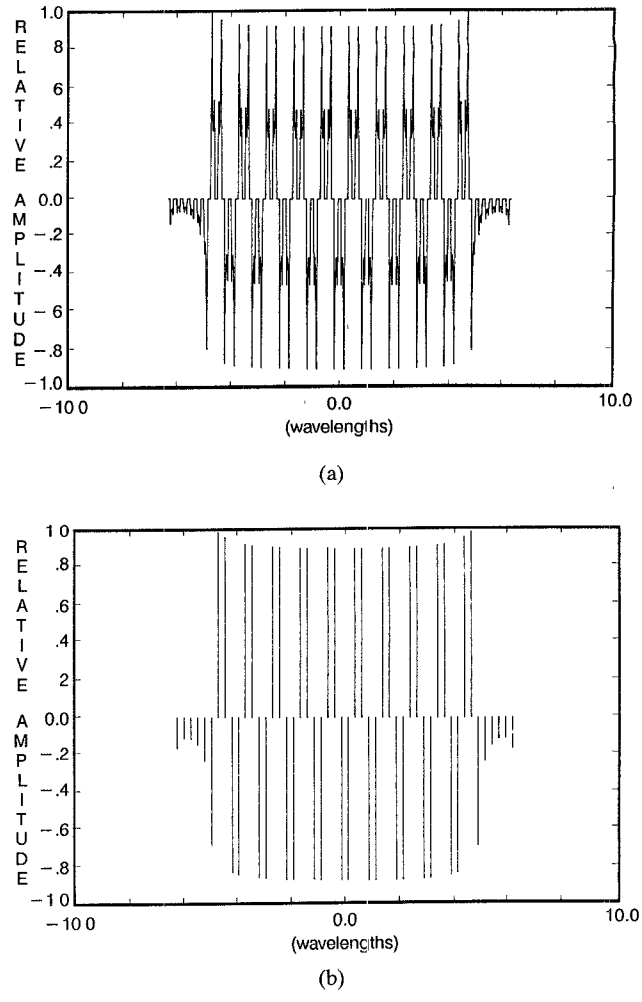

Fig. 11. Comparison of the charge distribution results of analysis for (a) the case of eight samples/period versus (b) using only a single sample/period.

The solution to the electrostatic charge distribution may now be obtained using (9) and (15).

The Green's function method has been exercised on a 10 wavelength, quadrature-sampled uniform transducer. The normalized charge distributions for a 50 percent metallization ratio are shown in Fig. 11 for sampling rates of 8 points/period and 1 sample point/period. The fundamental frequency responses for this array for metallization ratios of 25 percent, 50 percent, and 75 percent corresponding to 8 sample points/period as well as 1 sample point/period are shown in Fig. 12. The case of 1 sample/period required 1/64 the computation time as compared to the case of 8 samples/periods.

Given the electroacoustic response, calculation of the transducer's equivalent circuit requires that the acoustic conductance, acoustic susceptance, static capacitance, and parasitic electrode conductance be determined. The parasitic electrode conductance is a lumped element representation of the thin-film resistance present in each electrode.

The acoustic conductance is calculated from material parameters and the electrostatic charge distribution present on the array. The conductance of a SAW transducer

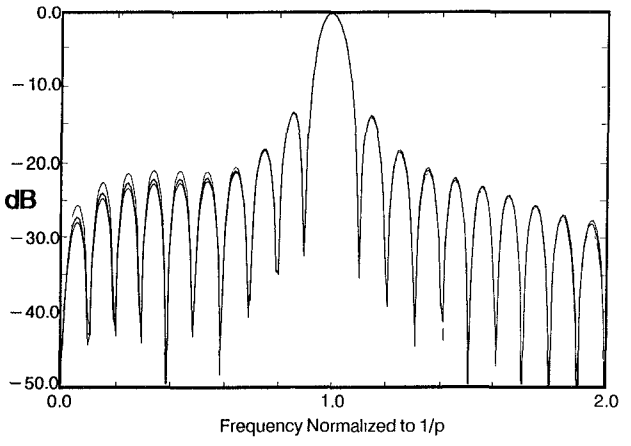

(a)

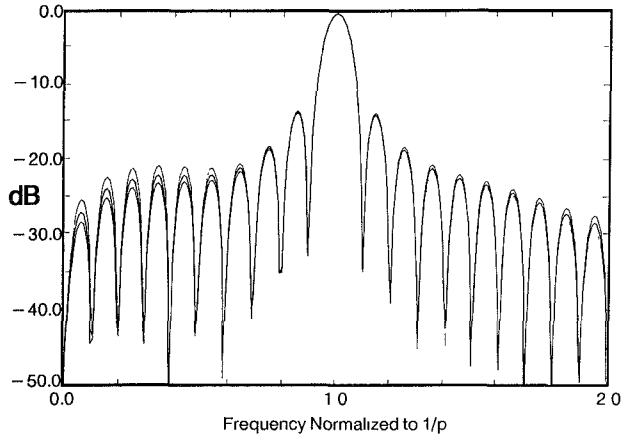

(b)

Fig. 12. Comparison of the frequency response results of analysis for (a) the case of eight samples/period versus (b) using only a single sample/period.

with uniform length taps is given by

$$G_a(w) = G_s\left|A_f(\omega)Q_f(\omega)\right|^2. \tag{16}$$

Here G_s is the conductance that a single positive polarity electrode in an infinite array of grounded electrodes would generate and is defined by [2]

$$G_s = 8k^2C_sWf_0 \tag{17}$$

where

W width of the transducer,
f_0 synchronous frequency of the structure $= p/v_s$.

For apodized transducers all electrodes are not of the same length and therefore (16) may not be used. For this case the transducer must be channelized for the purpose of evaluating the conductance of the device [2], [26]. The conductance for each channel of the device is then evaluated individually and the complete transducer conductance is obtained by using superposition.

The acoustic susceptance is calculated directly from the acoustic conductance via the Hilbert transform [1], [2] as

$$B_a(\omega) = G_a(\omega) * -1/\pi\cdot\omega. \tag{18}$$

The most efficient method for implementing the convolution is to make use of the fast Fourier transform.

$$B_a(\omega) = \mathrm{FFT}^{-1}\{-j\cdot\mathrm{sgn}(t)\cdot\mathrm{FFT}[G_a(\omega)]\}. \tag{19}$$

The static capacitance of the transducer is calculated using the results of the charge superposition analysis [1], [3], [4]. The total charge on the mth electrode of the infinite structure in Fig. 8 is given by [1], [4]

$$q_{fm} = 2C_s\int_0^1 \frac{\sin(\pi s)\cdot\cos(2\pi ms)}{P_{-s}[\cos(\pi a/p)]}P_{-s}[\cos(\pi a/p)]\,ds. \tag{20}$$

The electrode corresponding to $m = 0$ is the electrode with the nonzero potential applied to it.

This integral may be implemented as a fast Fourier transform as

$$q_{fm} = 2C_s\,\mathrm{FFT}\left[\frac{\sin(\pi s)}{P_{-s}[\cos(\pi a/p)]}P_{-s}[\cos(\pi a/p)]\right]. \tag{21}$$

The variable s is the frequency variable varying from 0 to 1 and m is the space variable, an integer varying from 0 to the number of points used in the transform. Therefore, q_{fm} will be the mth element of the resulting array. Given that the number of unique points resulting from the FFT is M and the number of electrodes used to define the array factor is N, the charge on the nth electrode may be calculated from

$$q_n = \sum_{m=1}^{M}(2W_n - W_{n-m} - W_{n+m})q_{fm}. \tag{22}$$

From the charges on each electrode the capacitance of the transducer may be calculated as

$$C_t = \sum_{n=1}^{N}|q_n|/2. \tag{23}$$

Power losses associated with the device must also be modeled. The first of these losses to be modeled is that attributed to the finite resistance of the electrodes. This loss is modeled as a lumped resistance. The parasitic electrode resistance may be calculated using [1]

$$R_e = (r_e/3)\frac{\sum_{n=1}^{N} q_n}{\sum_{n-1}^{N} A_nq_n}. \tag{24}$$

The loss attributed to this resistance at center frequency ω_0 may be calculated as $10\log(R_eG_a(\omega_0))$ dB.

Another loss term which can be significant in transducers which are weighted using apodization in apodization loss [27]. Apodization loss is a measure of the electroacoustic conversion efficiency of a SAW transducer. Apodization loss may be evaluated analytically as

$$\text{Apodization loss} = 10\log\left[\frac{\left[\int_0^W H(\omega, y)\,dy\right]^2}{W\cdot\int_0^W|H(\omega, y)|^2\,dy}\right] \tag{25}$$

where W equals the acoustic beam width and y is the transverse direction to the wave propagation.

In implementation, apodization loss may be calculated from quantities which are already known, thereby avoiding the integral in (25). Since the power radiated at center frequency is directly related to the conductance of the transducer at center frequency, apodization loss may be calculated from $G_a(\omega_0)$ as

$$\text{Apodization loss} = 10\log\left\{\frac{G_a(\omega_0)}{G_s \cdot |A_f(\omega_0)Q_f(\omega_0)|^2}\right\}. \quad (26)$$

A frequency span for the predicated complete analysis of the SAW filter's frequency response over the range of dc to the sampling rate of the time impulse response is obtained using the FFT algorithm.

Due to the number of channels used in analyzing each SAW transducer (usually 25 to 100), the time required for analysis is dominated by the FFT and not the general network analysis. Therefore it is desirable to reduce the number of points included in the analysis; however, this degrades the frequency-domain resolution. This limitation requires the implementation of a method by which the number of points may be decreased without sacrificing frequency-domain resolution. This may be accomplished by analyzing the SAW transducer with a minimal number of points as dictated by the transducer's time impulse response length and then augmenting additional points in the time domain in order to obtain the desired resolution in the frequency domain. The frequency response may then be obtained by performing an FFT. This procedure results in a fourfold to tenfold reduction in CAD time without losing either accuracy in the analysis or the frequency plots.

From the previous derivations, the complete, frequency-dependent SAW circuit model parameters are determined based on a unified charge superposition theory. All filters are constructed with two transducers, and in the implementation of bidirectional SAW filters multiple acoustic transitions result from electrical regeneration of received signals. These multiple transitions result in an amplitude and phase ripple through the passband of the filter. In order to minimize the magnitude of this ripple the device is usually mismatched. In the case of high loss, a relatively simple approximation can be made to model the effects of triple transit. This model is expressed analytically as

$$H(\omega) = \frac{H_1(\omega)H_2(\omega)e^{-j\omega\tau}}{1-0.5\left[H_1(\omega)H_2(\omega)e^{-j\omega\tau}\right]} \quad (27)$$

where

$H_1(\omega)$ transducer #1 frequency transfer function,
$H_2(\omega)$ transducer #2 frequency transfer function,
τ the acoustic filter delay.

With the addition of the triple transit analysis and transducer analysis, the complete SAW filter response can be simulated.

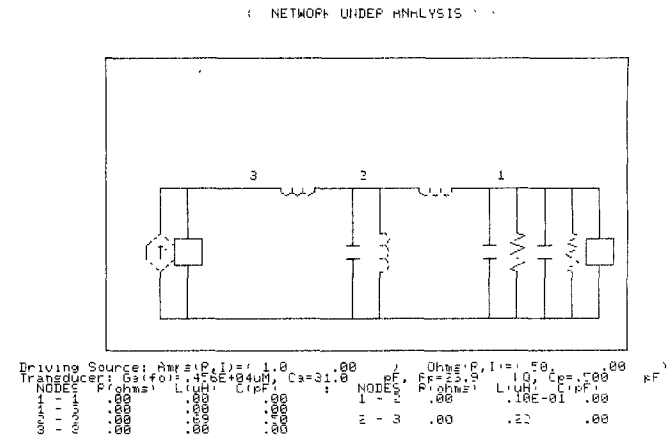

Fig. 13. Display of the complete electrical equivalent circuit model used to analyze a transducer, parasitic elements, and matching elements.

IV. Electrical Network Effects

The device analysis must be capable of inclusion of the effects of SAW device substrate parasitics, packaging parasitics, and external network effects. The most efficient way to accomplish this is to include network analysis capability in the CAD system. The complete electrical interactions can be predicted having extracted a lumped parameter equivalent circuit from the SAW device characteristics, and analyzing it as a node in a general network, which has the parasitic and external elements included.

With the knowledge of the equivalent network, the system can automatically calculate matching components. The CAD system defines a nodal network matrix which solves for the node voltages over broad band frequencies using Gaussian elimination routines. A typical example network simulation is shown in Fig. 13.

From the previous analysis of the electroacoustic response, the SAW equivalent circuit, and network interactions, calculation of the complete transducer response is achieved. Based on this approach, important transducer parameters versus frequency are extracted, such as input impedance, reflection coefficient, and mismatch loss.

V. Experimental Verification

A real-time SAW CAD personal-computer-based system has been implemented based on the design methods and analysis techniques described in this paper. This system is called SAWCAD-PC. A bidirectional, wide-band, low-shape-factor SAW filter designed by this system has been fabricated for the purpose of verifying the analysis techniques presented. The filter was designed on 128° YX $LiNbO_3$ having a center frequency of 60 MHz and an acoustic beam width of 35 λ_0. A multistrip coupler was used which allowed both transducers to be weighted using a slanted apodization pattern across the beam. The device was designed for a 6 MHz–6 dB bandwidth and a shape factor of 1.15. Using these parameters, the filter was designed using the cosine series superposition technique previously discussed.

A comparison of the predicted and experimental conductance and Hilbert transform susceptance is shown in

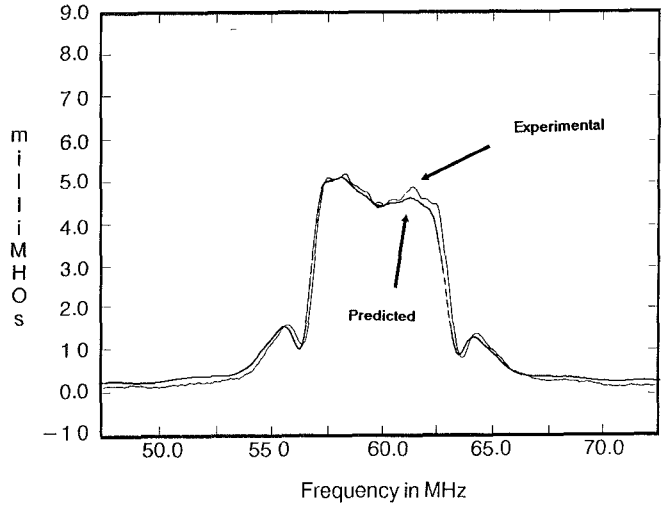

(a)

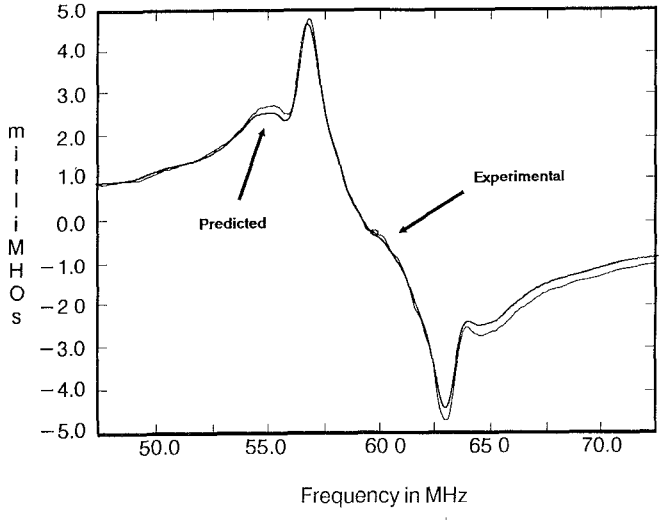

(b)

Fig. 14. Comparison of the CAD system's predicted and experimentally measured acoustic admittance for the input transducer. (a) Acoustic conductance. (b) Acoustic susceptance.

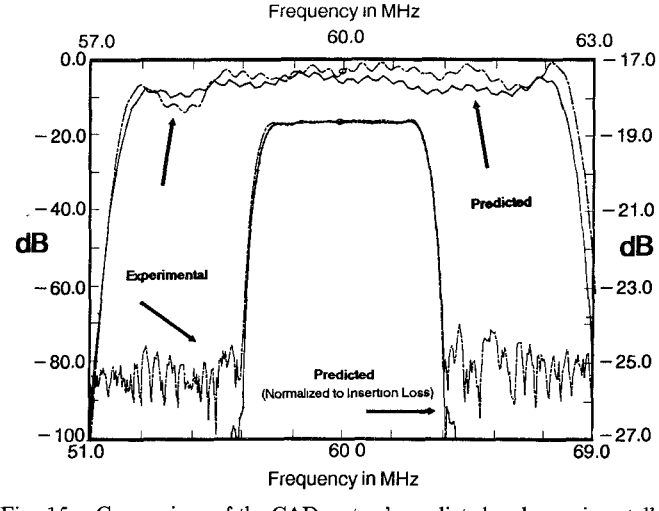

Fig. 15. Comparison of the CAD system's predicted and experimentally measured passband frequency response.

```
ucf-coe-ssds1                    SAWCAD-PC                    04-09-87   2 43 pm

                          SYSTEM INFORMATION

DISK FILES> last input  c523 t11                last output   ---- NONE ----
SYS DATA  > type  Time                          number of data samples  1024
NETWORK   > number of nodes    1                source node    1

                  Transducer Model Design Information

Tap sum = 16 89      Vector Tap sum = 10 78      Tap Squared sum = 9 264
Acoustic conduct  = 4416 3     umhos  Electrode capac   = 31, 028     pf
Thin film conduct = 41 860     umhos  Thin film resist  =  23889E-01 MOhms
Thin film loss    =  4097E-01  dB     Apodization loss  =   7796      dB
Input admittance  conductance = 4 48     mmhos, susceptance = 11 3     mmhos
Input impedance   resistance  = 30 0     Ohms,  reactance   =-76 4     Ohms
S11               real        =- 348           imaginary    =  624
Magnitude of S11              =  714         Mismatch loss  = 3 09
Transducer Qo                 = 2 54         Total BDT loss = 6 91

                    PRESS <enter> to continue
```

(a)

Parameter	SAWCAD-PC	Experiment	%Error
Ins. Loss	13.9 dB	17.3 dB	20
Gin(fo)	4.42 mMhos	4.78 mMhos	8
Bin(fo)	11.3 mMhos	13.0 mMhos	15
6 dB	5.85 MHz	5.85 MHz	0
40 dB	6.9 MHz	6.88 MHz	-.3
Out of Band Rejection	> 73 MHz	> 58MHz	-20
Shape Factor	1.18	1.18	0
Center Freq.	60 MHz	60 MHz	0
Passband Slope	0.65 dB	0.60 dB	-8

(b)

Fig. 16. (a) Actual PC display during calculation of the input transducer's equivalent circuit model. (b) Comparison of predicted and measured filter performance parameters.

Fig. 14. Fig. 15 shows a comparison of the theoretically predicted and experimental frequency bandpass responses for the filter. Correlation between experimental and the SAWCAD-PC analysis is excellent. The analysis of the device required less than 20 minutes on an PC-AT with a math coprocessor. Fig. 16(a) shows a display of the input transducer's electrical parameters at center frequency as displayed on the AT screen during the analysis session. Device parameters from the CAD system and several corresponding measurements taken from an HP 3577 network analyzer are shown in Fig. 16(b). The most significant error is in the predicted insertion loss. The current CAD system does not model the multistrip coupler effects and it is believed that an inefficient coupler was designed which caused increased error. The addition of the multistrip coupler analysis will be added in the future to predict these effects.

V. Conclusions

The existing literature on SAW modeling has been used as a base to develop a compatible, real-time, and accurate enhanced set of models for CAD implementation. All dominant surface acoustic wave effects have been included in a system whose architecture allows for the inclusion of higher order effects when appropriate models are developed. For example, diffraction models have been developed which appear computationally feasible and compatible with the present system [28], [29]. However, it is doubtful that diffraction analysis can be performed on the order of seconds for general filter design. For most conventional transducer designs, interelectrode mechanical reflections lie well outside the frequency band of interest, which does not distort the analysis approaches presented. Bulk wave and other non-SAW mode radiation can impact

the desired frequency response; however, choice of proper substrate and manufacturing techniques are used to minimize these effects. Also, the abrupt endings of the electrodes in the longitudinal and transverse directions to SAW propagation cause effects which are not easily implementable in a real-time system and represent a small second-order effect [30].

The development of a personal-computer-based integrated SAW CAD design and analysis system for bidirectional filter applications has been shown. The system's performance has been demonstrated via an analysis example. Development of this CAD system is continuing on three levels concurrently. At the model level, higher order effects of SAW propagation and electroacoustic interactions are being modeled. At the device level, models for other devices such as multiphase transducers and multistrip couplers are being developed. At the design level, a design automation system (SAW compiler) is being developed using the design and analysis modules of the CAD system with an automation shell written in PROLOG.

ACKNOWLEDGMENT

The authors would like to thank the members of the Solid State Devices and Systems Laboratory at the University of Central Florida. Many student members have contributed to the software development and verification tools which were presented in this paper.

REFERENCES

[1] D. P. Morgan, *Surface-Wave Devices for Signal Processing.* New York: Elsevier, 1985.

[2] C. S. Hartman, D. T. Bell, and R. C. Rosenfeld, "Impulse model design of acoustic surface wave filters," *IEEE Trans. Microwave Theory Tech.*, vol. MTT-21, pp. 162–175, 1973.

[3] S. Datta, B. J. Hunsinger, and D. C. Malocha, "A generalized model for periodic transducers with arbitrary voltages," *IEEE Trans. Sonics Ultrason.*, vol. SU-26, pp. 235–242, 1979.

[4] S. Datta and B. J. Hunsinger, "Element factor for periodic transducers," *IEEE Trans. Sonics Ultrason.*, vol. SU-27, pp. 42–44, 1980.

[5] W. R. Smith, H. M. Gerard, J. H. Collins, T. M. Reeder, and H. J. Shaw, "Analysis of interdigital surface wave transducers by use of an equivalent circuit model," *IEEE Trans. Microwave Theory Tech.*, vol. MTT-17, pp. 856–864, 1969.

[6] W. R. Smith and W. F. Pedler, "Fundamental and harmonic frequency circuit-model analysis of interdigital transducers with arbitrary metallization ratios and polarity sequences," *IEEE Trans. Microwave Theory Tech.*, vol. MTT-23, pp. 853–864, 1975.

[7] F. G. Marshall and E. G. S. Paige, "Novel acoustic surface wave directional coupler with diverse applications," *Electron. Lett.*, vol. 7, pp. 460–464, 1971.

[8] R. H. Tancrell and M. G. Holland, "Acoustic surface wave filters," *Proc. IEEE*, vol. 59, pp. 393–409, 1971.

[9] M. Hikita, Y. Kinoshita, H. Kojima, and T. Tabuchi, "Phase weighting for low loss SAW filters," in *IEEE Ultrason. Symp. Proc.*, 1980, pp. 308–312.

[10] M. Hikita, Y. Kinoshita, H. Kojima, and T. Tabuchi, "800 MHz low loss SAW filter using new phase weighting," in *IEEE MTT-S Microwave Symp. Dig.*, 1982, p. 46.

[11] C. S. Hartmann, "Weighting interdigital surface wave transducers by selective withdrawal of electrodes," in *IEEE Ultrason. Symp. Proc.*, 1973, pp. 423–426.

[12] D. C. Malocha, S. Datta, and B. J. Hunsinger, "Tap weight enhancement for broad-band filters," *IEEE Trans. Sonics Ultrason.*, vol. SU-25, pp. 51–54, 1978.

[13] K. R. Laker, E. Cohen, T. L. Szabo, and J. A. Pustaver, "Computer-aided design of withdrawal-weighted SAW bandpass filters," *IEEE Trans. Circuits Syst.*, vol. CAS-25, pp. 241–251, 1978.

[14] C. F. Vasile, "A numerical Fourier transform technique and its application to acoustic surface wave bandpass filter synthesis and design," *IEEE Trans. Sonics Ultrason.*, vol. SU-21, pp. 7–11, 1974.

[15] M. D. Adamo and C. F. Vasile, "Experimental verification of a new surface elastic wave bandpass filter synthesis technique," in *IEEE Ultrason. Symp. Proc.*, 1976, pp. 433–436.

[16] C. D. Bishop and C. D. Malocha, "Non-iterative design of SAW bandpass filters," in *IEEE Ultrason. Symp. Proc.*, vol. 1, 1984, pp. 18–21.

[17] D. C. Malocha and C. D. Bishop, "The classical truncated cosine series functions with applications to SAW filters, *IEEE Trans. Ultrason., Ferroelec. Freq. Contr.*, vol. UFFC-34, pp. 75–85, 1987.

[18] J. H. McClellan and T. W. Parks, "A uniform approach to the design of optimum FIR linear-phase digital filters," *IEEE Trans. Circuit Theory*, vol. CT-20, pp. 697–701, 1973.

[19] J. H. McClellan, T. W. Parks, and L. R. Rabiner, "A computer program for designing optimum FIR linear-phase digital filters," *IEEE Trans. Audio Electroacoust.*, vol. AU-21, pp. 506–526, 1973.

[20] R. Rabiner and B. Gold, *Theory and Application of Digital Signal Processing.* Englewood Cliffs, NJ: Prentice-Hall, 1975.

[21] K. A. Ingebrigtsen, "Surface waves in piezoelectrics," *J. Appl. Phys.*, vol. 40, pp. 2681–2686, 1969.

[22] C. S. Hartman and B. G. Secrest, "End effects in interdigital surface wave transducers," in *Proc. IEEE Ultrason. Symp.*, 1972, pp. 413–416.

[23] R. C. Peach, "A general approach to the electrostatic problem of the SAW interdigital transducer," *IEEE Trans. Sonics Ultrason.*, vol. SU-28, pp. 96–105, 1981.

[24] R. F. Milson, N. H. C. Reilly, and M. Redwood, "Analysis of generation and detection of surface and bulk acoustic waves by interdigital transducers," *IEEE Trans. Sonics Ultrason.*, vol. SU-24, pp. 147–166, 1977.

[25] D. P. Morgan, "Quasi-static analysis of generalized SAW transducers using the Green's function method," *IEEE Trans. Sonics Ultrason.*, vol. SU-27, pp. 111–123, 1980.

[26] R. H. Tancrell and M. G. Holland, "Acoustic surface wave filters," *Proc. IEEE*, vol. 59, pp. 393–409, 1971.

[27] R. A. Waldron, "Power transfer factors for nonuniformly irradiated interdigital piezoelectric transducers," *IEEE Trans. Sonics Ultrason.*, vol. SU-19, pp. 448–453, 1972.

[28] M. Roberts, "Diffraction modelling for SAW devices on anisotropic substrates," M.S. thesis, University of Central Florida, 1987.

[29] I. Stribel, "SAW diffraction compensation for $LiNbO_4$," M.S. thesis, Carleton University, Ottawa, Canada, 1984.

[30] R. S. Wagers, "Analysis of finite width interdigital transducer excitation profiles," *IEEE Trans. Sonics Ultrason.*, vol. SU-26, pp. 105–111, 1979.

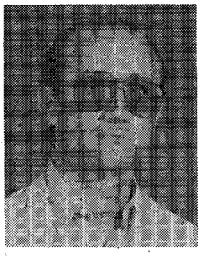

Samuel M. Richie (S'79–M'81) was born in Campton, KY, on May 19, 1958. He received the B.S.E. degree and the M.S.E. degree in electrical engineering from the University of Central Florida in 1980 and 1983, respectively. He is currently an electrical engineering instructor at the University of Central Florida, where he is finishing work on the Ph.D. degree.

While at the university he has worked on computer-aided design and analysis of both bidirectional and unidirectional SAW filter technology and previous to that worked on advanced concepts in point scanning computer image generation for simulation. Mr. Richie is a member of Eta Kappa Nu and Tau Beta Pi.

Benjamin P. Abbott (S'84–M'86) received the B.S.E. and M.S.E. degrees in electrical engineering from the University of Central Florida, Orlando, in 1984 and 1986, respectively.

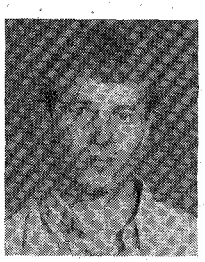

His research efforts have included the analysis of SAW bidirectional and three-phase apodized transducers as well as the development of a broad-band diffraction analysis technique for general anisotropic substrates. He is currently pursuing the Ph.D. degree at the University of Central Florida. His doctoral work concentrates on the design and analysis of unidirectional transducer technologies, including multiple- as well as single-phase unidirectional transducers.

✠

Donald C. Malocha (S'69–M'74–SM'84) was born in Chicago, IL, on October 17, 1950. He received the B.S. degree in electrical engineering and computer science, and the M.S. and Ph.D. degrees in electrical engineering from the University of Illinois, Urbana, in 1972, 1974, and 1977, respectively.

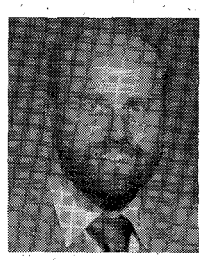

After one year as a Research Associate in the SAW group of Illinois's Coordinated Sciences Laboratory, he joined the Wave Electronics Branch of the Corporate Research Laboratory of Texas Instruments, Inc., Dallas, in 1978 as a Member of the Technical Staff. While at Texas Instruments, he was involved in SAW bidirectional and unidirectional transducer development, the SAW air-gap and elastic convolver programs, and SAW CAD techniques. In 1980, he joined Sawtek, Inc., Orlando, FL, as manager of Advanced Product Development. While at Sawtek he was engaged in SAW multiphase unidirectional analysis and design, SAW production filter designs, high-speed testing and data acquisition, and beamwidth compression convolver design. In 1982, he joined the University of Central Florida, where he is currently an Associate Professor in the Electrical Engineering and Communications Sciences Department and is group leader of the Solid State Devices and Systems Laboratory. His current interests are in SAW technology, CAD techniques, microelectronic devices, and communication systems.

Dr. Malocha is a member of the American Vacuum Society, Eta Kappa Nu, and Tau Beta Pi. He currently holds three patents.